

Room-Temperature Continuous-Wave Quantum Cascade Lasers Grown by MOCVD Without Lateral Regrowth

Zhijun Liu, Daniel Wasserman, Scott S. Howard, Anthony J. Hoffman, Claire F. Gmachl, *Senior Member, IEEE*, Xiaojun Wang, Tawee Tanbun-Ek, Liwei Cheng, and Fow-Sen Choa, *Senior Member, IEEE*

Abstract—We report on room-temperature continuous-wave (CW) operation of $\lambda \sim 8.2 \mu\text{m}$ quantum cascade lasers grown by metal-organic chemical vapor deposition without lateral regrowth. The lasers have been processed as double-channel ridge waveguides with thick electroplated gold. CW output power of 5.3 mW is measured at 300 K with a threshold current density of 2.63 kA/cm^2 . The measured gain at room temperature is close to the theoretical design, which enables the lasers to overcome the relatively high waveguide loss.

Index Terms—Continuous-wave (CW) lasers, midinfrared, quantum cascade (QC) lasers, semiconductor lasers.

I. INTRODUCTION

QUANTUM cascade (QC) lasers are promising and influential midinfrared light sources with potential for applications as varied as chemical sensing, wireless communication, and counter-measures. Since their first demonstration in 1994 [1], constant and significant performance improvements have been made for QC lasers through improved laser design, material growth, and packaging. Up to now, room-temperature continuous-wave (CW) operation, an important milestone for compact noncryogenic laser sources, has been demonstrated for QC lasers grown by solid source molecular beam epitaxy (MBE) or gas-source MBE at wavelengths of ~ 9.1 and $4\text{--}6 \mu\text{m}$ [2]–[7]. Metal-organic chemical vapor deposition (MOCVD) has recently attracted research interest because it is a technology preferred by industry and is promising for the commercialization of QC lasers [8]. MOCVD has been reported as a high-performance QC laser growth technique, first with low threshold pulsed operation [9], and very recently, room-temperature CW operation of an MOCVD-grown $\sim 7.2\text{-}\mu\text{m}$ QC laser and an MOCVD-grown $\sim 5.1\text{-}\mu\text{m}$ strained QC laser using a buried heterostructure design [10], [11]. In this letter, we report on an MOCVD-grown room-temperature CW QC laser at $\lambda \sim 8.2 \mu\text{m}$ without buried

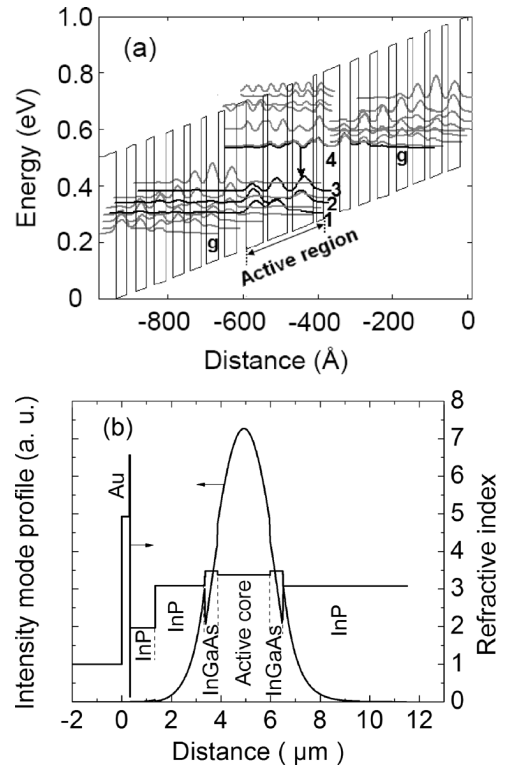


Fig. 1. (a) Portion of the conduction band diagram and the moduli squared of the relevant wave functions of a $\sim 8.2\text{-}\mu\text{m}$ QC laser with a four quantum-well active region based on a two phonon resonance. An electric field of 51 kV/cm is applied. The arrow indicates the laser transition. (b) Intensity profile of the fundamental mode, layer structure, and profile of the real part of the refractive index of the dielectric waveguide used.

heterostructure. The laser is processed as a double-channel ridge waveguide with thick electroplated gold on top, allowing the omission of the more complex lateral InP regrowth step.

II. LASER DESIGN AND FABRICATION

The laser active region is based on a two-phonon resonance design. The layer sequence (in \AA) of one period of active region and injector is **44/18/9/57/11/54/12/45/25/34/14/33/13/32/15/31/19/29/23/27/25/27**, where $\text{In}_{0.52}\text{Al}_{0.48}\text{As}$ barrier layers are in bold, $\text{In}_{0.53}\text{Ga}_{0.47}\text{As}$ well layers are in roman, and the n-doped ($2 \times 10^{17} \text{ cm}^{-3}$) layers are *underlined*. The electron energy band diagram is shown in Fig. 1(a). The energy of the laser transition between levels 4 and 3 is designed as 154 meV ,

Manuscript received February 22, 2006; revised April 7, 2006. This work was supported in part by the Defense Advanced Research Projects Agency (DARPA) L-PAS.

Z. Liu, D. Wasserman, S. S. Howard, A. J. Hoffman, and C. F. Gmachl are with the Department of Electrical Engineering and the Princeton Institute for the Science and Technology of Materials, Princeton University, Princeton, NJ 08544 USA (e-mail: cgmachl@princeton.edu).

X. Wang and T. Tanbun-Ek are with AdTech Optics, City of Industry, CA 91748 USA.

L. Cheng and F.-S. Choa are with the Department of Computer Science and Electrical Engineering, University of Maryland, Baltimore, MD 21250 USA.

Digital Object Identifier 10.1109/LPT.2006.877006

and levels 1, 2, and 3 are each separated by about one optical phonon energy. The relatively large energy separation between level 3 and the ground state of the next down stream injector (147 meV) is intended to suppress the thermal back filling effect. The lifetime of the upper laser level is designed as $\tau_4 = 2.11$ ps, and that of lower laser level is $\tau_3 = 0.22$ ps. The dipole matrix element z_{43} is 1.8 nm.

Thirty-five periods are used as the active core and sandwiched between two 0.5- μm -thick n-doped ($5 \times 10^{16} \text{ cm}^{-3}$) $\text{In}_{0.53}\text{Ga}_{0.47}\text{As}$ layers. The upper cladding layers consists of 2- μm -thick n-doped ($1 \times 10^{17} \text{ cm}^{-3}$) InP, followed by a 1- μm -thick n⁺-doped ($8 \times 10^{18} \text{ cm}^{-3}$) InP cap layer. The calculated intensity profile of the fundamental mode is shown in Fig. 1(b). The waveguide loss α_W is calculated as 6.6 cm^{-1} , and the confinement factor Γ is 0.67.

The double-channel ridge waveguide lasers were fabricated by conventional wet-chemical etching. A 0.3- μm -thick Si_xN_y layer was deposited for side-wall insulation. After evaporation of Ti–Au (30/300 nm) for the top contact, a > 10 - μm -thick gold layer was electroplated around the laser ridge for efficient heat transfer. To facilitate cleaving, small gaps were left in the thick electroplated gold layer. After the wafer was thinned to $\sim 150 \mu\text{m}$, the back Ge–Au (15/300 nm) contact was evaporated. The laser was mounted epilayer-up to a copper submount with In solder, and wire bonded. Finally, the back facet was high-reflection (HR) coated with SiO_2 –Ti–Au– SiO_2 (400/15/100/100 nm).

III. LASER CHARACTERIZATION

For testing, the lasers were loaded onto a cryostat, with the temperature measured on the cryostat cold finger next to the laser mount. Fig. 2(a) shows the CW light–current curves of an HR-coated, 8- μm -wide, 3.5-mm-long QC laser at different heat sink temperatures. The voltage–current curve at 300 K is also given. A CW optical output power of 5.3 mW is obtained with a threshold current of 0.73 A (corresponding to $J_{\text{th}} = 2.63 \text{ kA/cm}^2$) at 300 K. The typical emission spectrum at 300 K is given by the inset of Fig. 2(a). The lasing wavelength is $\sim 8.2 \mu\text{m}$. Fig. 2(b) shows the threshold current density of the laser as a function of the heat sink temperature for both pulsed and CW operation. For pulsed operation, the threshold current density increased from 1.21 kA/cm^2 at 240 K to 2.26 kA/cm^2 at 380 K. The CW threshold current density increased from 1.56 kA/cm^2 at 240 K to 3.2 kA/cm^2 at 315 K. The solid lines are the result of exponential fits $J_{\text{th}} = J_0 \exp(T/T_0)$. The extracted characteristic temperature T_0 is 217 K and 107 K for pulsed operation and CW operation, respectively. By comparing the two curves in Fig. 2(b), the temperature difference between laser active region and the heat sink can be deduced, and thus, the thermal resistance can be calculated by using the relation $R_{\text{th}} = (T_{\text{act}} - T_{\text{sink}})/(I_{\text{th}}V_{\text{th}})$, where T_{act} is the temperature of active region in CW operation, T_{sink} is the CW heat sink temperature, I_{th} is the threshold current, and V_{th} is the threshold voltage in CW operation. At 300 K, $\Delta T = T_{\text{act}} - T_{\text{sink}} = 95 \text{ K}$, $I_{\text{th}} = 0.73 \text{ A}$, $V_{\text{th}} = 9.33 \text{ V}$, and R_{th} is calculated as 13.9 K/W , which is close to the value reported for comparable QC lasers grown by MBE [3].

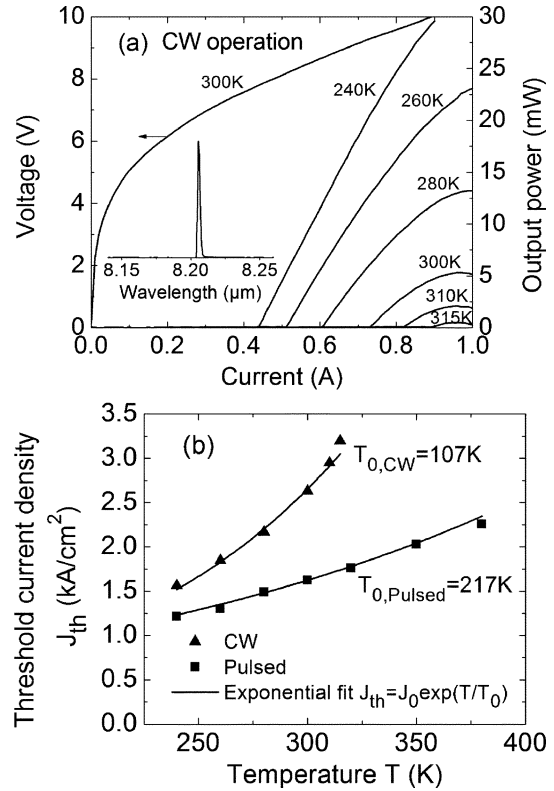


Fig. 2. (a) CW light–current curves of an HR-coated, 8- μm -wide, 3.5-mm-long QC laser at different heat sink temperatures. The voltage–current curve at 300 K is also given. The inset shows the laser spectrum at 300 K and 0.74 A. (b) Threshold current density as a function of the heat sink temperature in pulsed and CW operation (data points). The solid lines are the results of exponential fits $J_{\text{th}} = J_0 \exp(T/T_0)$. From 240 K to 380 K, $T_0 = 217 \text{ K}$ for pulsed operation, and from 240 K to 315 K, $T_0 = 107 \text{ K}$ for CW operation.

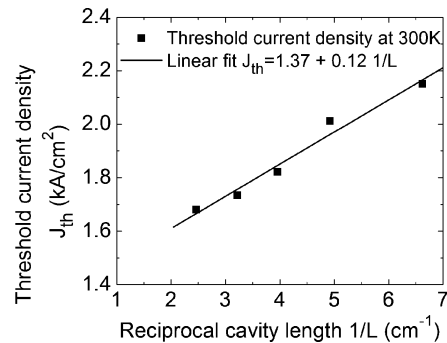


Fig. 3. Measured pulsed threshold current density versus reciprocal cavity length at 300 K. The solid line is the result of a linear least squares fit.

In order to better understand the lasing performance of the device, we used the “1/L” and Hakki–Paoli methods to measure gain and waveguide loss. Fig. 3 shows the plot of the pulsed threshold current density versus reciprocal cavity length at 300 K. From the linear fit curve, one deduces the waveguide loss α_W as 14.3 cm^{-1} , and the modal gain coefficient as 10.4 cm/kA . Fig. 4 shows the net modal gain as a function of the current density for two Fabry–Pérot QC lasers at 280 K by using the Hakki–Paoli method. The linear fit gives the waveguide loss of the 13.5- μm -wide laser as 14.5 cm^{-1} , which is in good agreement with the “1/L” method. A second 9- μm -wide laser

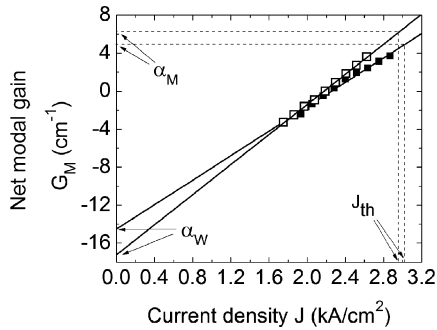


Fig. 4. Net modal gain G_M as a function of the current density J of a 2.53-mm-long 13.5- μm -wide QC laser (solid square) and a 2.03-mm-long 9- μm -wide QC laser (open square). The net modal gain is deduced from subthreshold emission spectra at 280 K. The solid line is the result of a linear least squares fit, which is $G_M = -14.5 + 6.43 J$ and $G_M = -17.23 + 7.92 J$ for the solid squares and open squares, respectively.

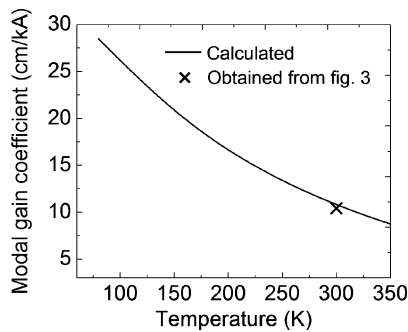


Fig. 5. Calculated modal gain coefficient as a function of temperature.

showed a higher waveguide loss, i.e., 17.2 cm^{-1} . These measured losses are significantly higher than the calculated value of 6.6 cm^{-1} obtained from a three-dimensional waveguide model. The discrepancy is likely caused by additional waveguide loss from scattering, and some absorption within the injector. More studies are needed to identify the true origins. Fig. 5 shows the theoretical modal gain coefficient as a function of temperature. The temperature-dependent measured luminescence linewidth (e.g., 13.6 meV at 80 K and 19.8 meV at 300 K) was used in this calculation. As can be seen, the measured modal gain coefficient 10.4 cm/kA at 300 K is very close to the designed value, i.e., 10.8 cm/kA.

It is finally interesting to examine the difference between this two-channel ridge waveguide laser and previously reported buried heterostructure QC lasers [2], [10], [11] with regards to waveguide loss and gain. The reported values of the waveguide loss of the buried heterostructure QC lasers at 9.1, 7.2, and 5.1 μm are 10, 6, and 9.7 cm^{-1} , respectively [2], [10], [11]. All are lower than that of our laser, likely due to the advantage of lateral InP regrowth. The modal gain coefficients at 300 K from [2], [10], and [11], using the relation $g\Gamma = (\alpha_W + \alpha_M)/J_{th}$, are deduced to be 4.8, 4.4, and 5.2 cm/kA, respectively. These values are approximately half of our measured gain coefficient of 10.4 cm/kA in Fig. 3. We attribute this difference to the more

“diagonal” laser transition in our design, which has a longer upper laser level lifetime. Therefore, the laser reported here has a higher gain but also a higher waveguide loss. With further optimization in the doping and waveguide structure, we believe it is possible to reduce the waveguide loss and improve the laser performance.

IV. CONCLUSION

We have demonstrated room-temperature CW operation of QC lasers grown by MOCVD using a straightforward double-channel ridge waveguide with thick electroplated gold on top. These MOCVD-grown QC lasers operate in CW at room temperature without buried heterostructure design. The measured gain is close to the theoretical value, and higher than that of previously reported buried heterostructure lasers, compensating for the higher waveguide loss.

ACKNOWLEDGMENT

The authors acknowledge the assistance of Dr. I. E. Trofimov with electroplating.

REFERENCES

- [1] J. Faist, F. Capasso, D. L. Sivco, C. Sirtori, A. L. Hutchinson, and A. Y. Cho, “Quantum cascade laser,” *Science*, vol. 264, pp. 553–556, 1994.
- [2] M. Beck, D. Hofstetter, T. Aellen, J. Faist, U. Oesterle, M. Ilegems, E. Gini, and H. Melchior, “Continuous wave operation of a midinfrared semiconductor laser at room temperature,” *Science*, vol. 295, pp. 301–305, 2002.
- [3] J. S. Yu, S. Slivken, A. Evans, L. Doris, and M. Razeghi, “High-power continuous-wave operation of a 6 μm quantum-cascade laser at room temperature,” *Appl. Phys. Lett.*, vol. 83, pp. 2503–2505, 2003.
- [4] A. Evans, J. S. Yu, S. Slivken, and M. Razeghi, “Continuous-wave operation of $\lambda \sim 4.8 \mu\text{m}$ quantum-cascade lasers at room temperature,” *Appl. Phys. Lett.*, vol. 85, pp. 2166–2168, 2004.
- [5] S. Blaser, D. A. Yarekha, L. Hvozdar, Y. Bonetti, A. Muller, M. Giovannini, and J. Faist, “Room-temperature, continuous-wave, single-mode quantum-cascade lasers at $\lambda \sim 5.4 \mu\text{m}$,” *Appl. Phys. Lett.*, vol. 86, pp. 041 109-1–041 109-3, 2005.
- [6] J. S. Yu, A. Evans, S. Slivken, S. R. Darvish, and M. Razeghi, “Short wavelength ($\lambda \sim 4.3 \mu\text{m}$) high-performance continuous-wave quantum-cascade lasers,” *IEEE Photon. Technol. Lett.*, vol. 17, no. 6, pp. 1154–1156, Jun. 2005.
- [7] J. S. Yu, S. R. Darvish, A. Evans, J. Nguyen, S. Slivken, and M. Razeghi, “Room-temperature continuous-wave operation of quantum-cascade lasers at $\lambda \sim 4 \mu\text{m}$,” *Appl. Phys. Lett.*, vol. 88, pp. 041 111-1–041 111-3, 2006.
- [8] V. Moreau, A. B. Krysa, M. Bahriz, L. R. Wilson, R. Colombelli, D. G. Revin, F. Julien, J. W. Cockburn, and J. S. Roberts, “Pulsed operation of long-wavelength ($\lambda \sim 11.3 \mu\text{m}$) MOVPE-grown quantum cascade lasers up to 350 K,” *Electron. Lett.*, vol. 41, pp. 1175–1176, 2005.
- [9] J. S. Roberts, R. P. Green, L. R. Wilson, E. A. Zibik, D. G. Revin, J. W. Cockburn, and R. J. Airey, “Quantum cascade lasers grown by metalorganic vapor phase epitaxy,” *Appl. Phys. Lett.*, vol. 82, pp. 4221–4223, 2003.
- [10] M. Troccoli, S. Corzine, D. Bour, J. Zhu, O. Assayag, L. Diehl, B. G. Lee, G. Hoffer, and F. Capasso, “Room temperature continuous-wave operation of quantum-cascade lasers grown by metal organic vapor phase epitaxy,” *Electron. Lett.*, vol. 41, pp. 1059–1060, 2005.
- [11] L. Diehl, D. Bour, S. Corzine, J. Zhu, G. Hoffer, B. G. Lee, C. Y. Wang, M. Troccoli, and F. Capasso, “Pulsed- and continuous-mode operation at high temperature of strained quantum-cascade lasers grown by metalorganic vapor phase epitaxy,” *Appl. Phys. Lett.*, vol. 88, pp. 041 102-1–041 102-3, 2006.